Original Article

MOLECULAR METABOLISM

Neurturin is a PGC-1α1-controlled myokine that promotes motor neuron recruitment and neuromuscular junction formation

Richard Mills [1,4], Hermes Taylor-Weiner [1,4], Jorge C. Correia [2], Leandro Z. Agudelo [2], Ilary Allodi [3], Christina Kolonelou [1], Vicente Martinez-Redondo [2], Duarte M.S. Ferreira [2], Susanne Nichterwitz [3], Laura H. Comley [3], Vanessa Lundin [1], Eva Hedlund [3], Jorge L. Ruas [2,*], Ana I. Teixeira [1,]**

ABSTRACT

Objective: We examined whether skeletal muscle overexpression of PGC-1α1 or PGC-1α4 affected myokine secretion and neuromuscular junction (NMJ) formation.

Methods: A microfluidic device was used to model endocrine signaling and NMJ formation between primary mouse myoblast-derived myotubes and embryonic stem cell-derived motor neurons. Differences in hydrostatic pressure allowed for fluidic isolation of either cell type or unidirectional signaling in the fluid phase. Myotubes were transduced to overexpress PGC-1α1 or PGC-1α4, and myokine secretion was quantified using a proximity extension assay. Morphological and functional changes in NMJs were measured by fluorescent microscopy and by monitoring muscle contraction upon motor neuron stimulation.

Results: Skeletal muscle transduction with PGC-1α1, but not PGC-1α4, increased NMJ formation and size. PGC-1α1 increased muscle secretion of neurturin, which was sufficient and necessary for the effects of muscle PGC-1α1 on NMJ formation.

Conclusions: Our findings indicate that neurturin is a mediator of PGC-1α1-dependent retrograde signaling from muscle to motor neurons.

Keywords Skeletal muscle; PGC-1α; Neurturin; Motor neuron; Myokine

1. INTRODUCTION

Peroxisome-proliferator-activated receptor γ coactivator-1α (PGC-1α) proteins are key regulators of mitochondrial biogenesis and energy metabolism [1] with important roles in the biology of skeletal muscle. Expression of PGC-1α coactivators in skeletal muscle is induced by exercise, in both rodents and humans, regulating many of the effects of exercise training. The PGC-1α gene has been recently found to encode for different splice variants [2]. Among these, the canonical PGC-1α1 form [3] as well as many of the more recently reported splice variants [4,5] have been shown to regulate oxidative metabolism including mitochondrial biogenesis, fiber-type switching, stimulation of fatty acid oxidation, angiogenesis, and resistance to muscle atrophy [6]. Interestingly, PGC-1α4 does not directly affect cellular bioenergetic processes but instead induces IGF-1 expression and represses myostatin, resulting in muscle hypertrophy and increased strength [2]. PGC-1α4 integrates resistance training with a gene program of muscle hypertrophy, while PGC-1α1 regulates skeletal muscles' adaptations to endurance exercise.

PGC-1α1 has been identified as a regulator of neuromuscular junction (NMJ) structure and activity [7,8]. It was initially noted that mice overexpressing PGC-1α1 in skeletal muscle (MCK-PGC-1α1) show reduced muscle-mass loss and maintain muscle fiber volume during denervation in comparison to wild-type controls [9]. Moreover, when MCK-PGC-1α1 mice are bred with a mouse model of Duchenne's Muscular Dystrophy (mdx mice), the resulting progeny exhibit improved muscle health and greater NMJ number and integrity [8]. Skeletal muscle PGC-1α1 affects NMJs by enhancing transcription of genes such as acetylcholine receptor (AChR) subunits, utrophin, ErbB2, rapsyn, and GABP, and by promoting AChR clustering [8]. Interestingly, ectopic or transgenic expression of PGC-1α1 in muscle fibers can convert motor neurons to a slow phenotype, suggesting that there is PGC-1α1-dependent retrograde signaling from muscle to motor neurons [10].

[1]Department of Medical Biochemistry and Biophysics, Karolinska Institutet, Scheeles väg 2, 171 77, Stockholm, Sweden [2]Molecular and Cellular Exercise Physiology, Department of Physiology and Pharmacology, Karolinska Institutet, von Eulers väg 8, 171 77, Stockholm, Sweden [3]Department of Neuroscience, Karolinska Institutet, Retzius väg 8, 17177, Stockholm, Sweden

[4] Co-first authors.

*Corresponding author. E-mail: jorge.ruas@ki.se (J.L. Ruas).

**Corresponding author. Division of Biomaterials, Department of Medical Biochemistry and Biophysics, Karolinska Institutet, Scheeles väg 2, 171 77, Stockholm, Sweden. E-mail: Ana.Teixeira@ki.se (A.I. Teixeira).

Received October 23, 2017 • Revision received October 31, 2017 • Accepted November 1, 2017 • Available online 7 November 2017

https://doi.org/10.1016/j.molmet.2017.11.001

To investigate how PGC-1α isoforms affect NMJs and the role of retrograde signaling during NMJ formation, we utilized an *in vitro* microfluidic NMJ model. NMJ models that involve simple co-culture of motor neurons and myotubes lack individual control of the micro-environmental cues received by these two cell types. Microfluidics allow for spatially defined control of cellular microenvironments [11]. For example, in a recent study by Zahavi et al. [12] a microfluidic NMJ co-culture system enabled the detection of spatially distinct aspects of GDNF signaling in motor neurons, showing promotion of NMJ formation at nerve terminals and cell survival in the soma. We used a similar microfluidic device to generate a functional *in vitro* NMJ, which allows for the specific manipulation of each cell type and control of the cellular microenvironment. Importantly, it allows for directional control of communication between motor neurons and muscle mediated by soluble factors. Using this model, we manipulated the levels of PGC-1α1 and PGC-1α4 in mouse myotubes and found that PGC-1α1 expression resulted in pre-synaptic and post-synaptic NMJ changes. Using a bioinformatics approach, combining gene array data and *in silico* prediction strategies, we identified the myokine (muscle-derived cytokine) neurturin, as a key component in PGC-1α1 mediated neurite recruitment to muscle.

2. MATERIALS AND METHODS

2.1. Cell culture

Primary satellite cells (myoblasts) were isolated, maintained and differentiated as previously described [2].

Hb9:GFP mESCs were generated and maintained as previously described [13,14]. mESCs were differentiated into motor neurons using an embryoid body (EB) protocol. mESCs were detached from culture plates by removing medium and adding TrypLE Express (Life Technologies) for 5 min at 37 °C. Single cells were then resuspended in mESC media (Supplemental Table 1), seeded in a 0.1% gelatin-coated dish and incubated for 30–60 min at 37 °C to remove contaminating mouse embryonic fibroblasts. Cells in suspension were removed and placed in a bacterial dish to initiate EB formation. After two days, EBs were split from one dish into four petri dishes containing differentiation medium (Supplemental Table 2) supplemented with 0.1 μM retinoic acid (Sigma R2625) and 0.5–1 μM of the smoothened agonist SAG (Merck). Medium was changed every 48 h. On day seven, the embryoid bodies were dissociated into single cell suspension using TrypLE Express and resuspended in differentiation medium containing 5 ng/ml BDNF and GDNF (R&D Systems 212-GD and 248-BD). Cells were counted and seeded in the microfluidic devices as described below.

2.2. Microdevice setup

Microdevices were plasma treated, attached to glass substrates and UV sterilized as per the user manual instructions (Xona Microfluidics SND150). Each device was designated a motor neuron (MN) culture compartment and a myotube culture compartment. Both cell culture compartments were initially coated in poly-L-ornithine (PLO, 0.01%) for 2 h at 37 °C. PLO was then removed and substrates were washed with PBS. 10 μg/ml Laminin (Sigma Aldrich L2020) was pipetted into the MN compartment, while 50 μg/ml of Collagen (Corning 354249) in combination with 10 μg/ml of Laminin were added to the muscle compartment. Devices were incubated overnight at 37 °C and then washed with PBS in preparation for cell seeding.

Myoblasts were harvested and seeded first. Myoblasts were resuspended at a density of 12×10^6 cells per ml and pipetted into the muscle culture compartment (12 μl); resulting in 144,000 myoblasts per device. Following myoblast seeding, motor neurons were harvested, and resuspended at a density of 15×10^6 cells per ml. Motor neurons were then pipetted into the MN compartment (12 μl); resulting in 180,000 MNs per device. Devices were incubated for 2 h at 37 °C to facilitate cell attachment, followed by addition of their respective medium to fill devices (motor neuron side: MN media containing 5 ng/ml of BDNF and GDNF, muscle side: DMEM/F12 containing 20% FBS (Supplemental Table 3)). Myoblast differentiation was initiated after 12–16 h, by adding myoblast differentiation medium (DMEM containing 5% horse serum (Supplemental Table 4)). Myoblasts were differentiated for 48 h to form multinucleated fibers, while the motor neurons were fluidically isolated and maintained in MN differentiation medium. Motor axons were then recruited across the microchannels using GDNF and BDNF. GDNF and BDNF at 20 ng/ml were added to the muscle compartment, in combination with fluid flow from the muscle to the motor neuron compartment using a 20 μl difference in volume between the compartments, resulting in neurite recruitment. After the neurites had contacted the myotubes, neuromuscular junctions were sustained with MN and muscle differentiation medium, respectively until day 10. Medium was replaced daily. Axonal growth into the muscle compartment was visualized and quantified using the Hb9-GFP reporter on a Leica DMI6000.

2.3. Testing of fluidic isolation

Fluidic isolation was tested using fluorescein isothiocyanate (FITC)-dextran (10 kDa) (Sigma Aldrich FD10S) as previously described [15]. Fluorescence was visualized on a Leica DMI6000.

2.4. Adenovirus mediated expression

Adenoviruses expressing PGC-1α1 [2], PGC-1α4 [2], GFP [2], NRTN shRNA (Vector Biolabs SKU#: shADV-266099), or scramble shRNA (Vector Biolabs) were generated as previously described or purchased. The viral titers for the NRTN shRNA and scramble shRNA adenoviruses were measured in HEK293 cells to be 3.27×10^{11} ifu/ml and 2.23×10^{11} ifu/ml, respectively. Differentiated myotubes were transduced with adenovirus within the muscle cell culture compartment for 8 h. This was performed under fluidic isolation to ensure that myotubes were selectively transduced (100 μl difference in volume between the compartments). GFP expression, in all conditions, was robustly observed 24–48 h following adenovirus treatment.

2.5. Stimulation and inhibition of neuromuscular junctions

We monitored muscle contractions in response to neuronal stimulation and NMJ inhibition. 50 mM KCl was flowed through the MN culture compartment, while under fluidic isolation, to depolarize motor neurons. Following KCl treatment, blocking of NMJs was performed using 8 μM tubocurarine chloride pentahydrate (Sigma Aldrich 93750). Video recordings were collected and muscle contractions analyzed using ImageJ.

2.6. Intracellular calcium measurements

To measure intracellular calcium levels, primary muscle cells were incubated for 20 min with 5 μM Fluo-3 AM (Invitrogen), a cell permeable fluorescent indicator of calcium concentration. Confocal images were collected before and after staining and the ratio of final to initial fluorescence was calculated using ImageJ.

2.7. Immunostaining

Cultures were fixed using 4% paraformaldehyde for 30 min at room temperature. Cultures were then washed with PBS, and treated with PBS containing 0.1% Triton X-100 and 3% bovine serum albumin (BSA)

to block non-specific binding and facilitate cell permeabilization. Primary antibodies were incubated with PBS containing 0.1% Triton X-100 and 3% BSA at 4 °C. Primary antibodies used for staining: Neurofilament (1:200; Sigma Aldrich N4142), Green Fluorescent Protein (1:500; Sigma Aldrich G6539). We then washed cultures with PBS and incubated them with secondary antibodies for 2 h at room temperature. Secondary antibodies used for staining: Alexa Fluor 488 Goat anti-Mouse (1:200; Life Technologies A11001), Alexa Fluor 633 Goat anti-Rabbit (1:200; Life Technologies A21070). α-Bungarotoxin Alexa Fluor 555 conjugate (1:1000; Life Technologies B35451) and 4′,6-diamidino-2-phenylindole (DAPI, 1:1000, Life Technologies D1307) were used to label acetylcholine receptors and cell nuclei, respectively. Alexa Fluor 488 Phallodin (1:50; Life Technologies A12379) was used to label filamentous actin. Images were taken on a Zeiss LSM700 and quantification of immunolabeling was performed using ImageJ. To quantify NMJ morphology, immunolabeled AChR aggregates and neurofilament were masked and overlayed to determine co-localization, aggregates above 0.5 μm^2 were considered NMJs.

2.8. MicroArray

Analysis of global gene expression profiles was performed on fully differentiated myotubes transduced with PGC-1α1 or GFP control (published dataset, GEO GSE42473 [2]). Differential gene expression was calculated using a two-sided unpaired Student's t-test with equal variance. From these gene sets, corresponding protein sequences were downloaded, and *in silico* prediction of secreted proteins was performed as previously described [16].

2.9. Proseek assays

To quantify the level of proteins in solution, we used a Proseek assay development kit (Olink Bioscience). Proseek assays were developed for Glial cell-derived neurotrophic factor (GDNF), Interleukin 15 (IL-15), Neurturin (NRTN) and Nerve growth factor (NGF) as per the user manual instructions. Briefly, the Proseek assay is based on Proximity Extension Assay technology. A pair of oligonucleotide labeled antibodies, Proseek probes (Proseek Probemaker A (93001) and Proseek probemaker B (93002)), are allowed to bind pair-wise to the target protein present in the sample in a homogeneous assay. When the two Proseek probes are in close proximity, a PCR target sequence is formed by a proximity dependent DNA polymerization event (Proseek assay reagents (93003)). The resulting sequence is subsequently detected and quantified using real-time PCR. 1 μl samples of conditioned media from PGC-1α1, PGC-1α4, and GFP-control treated myotubes were compared against a standard curve of known antigen (Figure S4). Antibody-related information for Proseek probes: GDNF (R&D Systems AF-212-NA), IL-15 (R&D Systems AF-447), NRTN (R&D Systems AF-477), NGF (R&D Systems AF-256-NA). Antigen related information to generate standard curves: GDNF (R&D Systems 212-GD), IL-15 (R&D Systems 447-ML), NRTN (R&D Systems 477-MN), NGF (R&D Systems 1156-NG).

2.10. Quantitative RT-Polymerase chain reaction (qRT-PCR)

500 ng RNA was incubated with amplification grade DNase I (Invitrogen cat # 18068015) and used to synthesize cDNA using the Applied Biosystems High-Capacity RNA-to-cDNA kit (cat # 4387406). The resulting cDNA was diluted 1:9 in water and analyzed using a 384-well ViiA 7 qPCR System (Applied Biosystems) and Power SYBR Green PCR Master Mix (Applied Biosystems cat # 4367659). TATA-binding protein (TBP) was used to normalize all data, which was plotted as a fold-change from controls. Primer sequences can be found in Supplemental Table 5.

2.11. Statistical analyses

All results are expressed as mean ± SEM. Statistical significance was determined by one-way ANOVA with Bonferroni's post-hoc tests, by Kruskal–Wallis tests with Dunns post-hoc tests (for non-Gaussian distributions), or unpaired two-tailed Student's t-test as appropriate. $P < 0.05$ was considered statistically significant.

3. RESULTS

3.1. Development of a functional *in vitro* NMJ model

To investigate how muscle PGC-1α coactivators affect motor neuron recruitment and neuromuscular junction formation, we developed an *in vitro* microfluidics-based model. Mouse primary myoblast-derived myotubes and mouse embryonic stem cell (mESC)-derived motor neurons were cultured in separate compartments, connected by microchannels, in microfluidic devices. These devices allow for on-demand unidirectional or bidirectional communication between the compartments, dependent on whether there is a difference in hydrostatic pressure between the respective compartments [15]. We confirmed that, in these devices, a higher volume of medium in one of the compartments leads to a small, sustained fluid flow towards the contralateral compartment, counteracting diffusion (Figure S1). In this way, unidirectional communication through the fluid phase was established from the first to the second compartment, keeping the first compartment under fluidic isolation.

During muscle differentiation, motor neuron cultures were kept in fluidic isolation from soluble signals originating from the muscle compartment (Figure 1*A* and *B*). A mESC line, engineered with an Hb9:GFP transgene [13,14], was used to allow the visualization of motor neurons (MNs) by GFP expression. The differentiation protocol used in this study, which relies on retinoic acid (RA) and the smoothened agonist SAG, generates both lateral motor column motor neurons that express FoxP1 and medial motor column motor neurons defined by Lhx3 expression [17]. The neurotrophic factors BDNF and GDNF promote motor neurite recruitment *in vitro* [18]. To validate the performance of the model with respect to soluble-factor mediated neurite recruitment, BDNF and GDNF were added to the muscle compartment two days after the onset of muscle differentiation. Unidirectional flow was established toward the motor neuron compartment, creating a chemotactic gradient. After six days of culture, neurites crossed the microchannels and contacted the myotubes (Figure 1*C* and *D*). The addition of BDNF and GDNF to the muscle compartment from day four promoted a greater than three-fold increase in the number of neurites crossing the center of the microchannels on day six (Figure 2*A* and *B*). On subsequent days, motor neurons extended axons, which branched and contacted multiple myotubes. At day ten, we confirmed the presence of neuromuscular junctions (NMJs) by staining with α-bungarotoxin, which binds acetylcholine receptors (AChRs) on myotubes. AChRs were observed to cluster and co-localize with GFP at the intersection of motor neurons and muscle fibers, indicative of NMJ formation (Figure 2*C*).

To investigate whether NMJs were functional, we monitored myotube contraction in response to motor neuron stimulation with potassium chloride (KCl), as well as NMJ inhibition using tubocurarine, an AChR antagonist. Using live microscopy, we identified regions where GFP positive motor neurons were in contact with myotubes that showed sustained and coordinated contractions (Movie S1 and S2). Stimulation of motor neurons with 50 mM KCl caused myotubes to contract with higher frequency than the spontaneous contractions observed prior to stimulation (Figure 2*D* and *E*, Movie S3). KCl was added to the motor neuron compartment while under fluidic isolation, ensuring that the

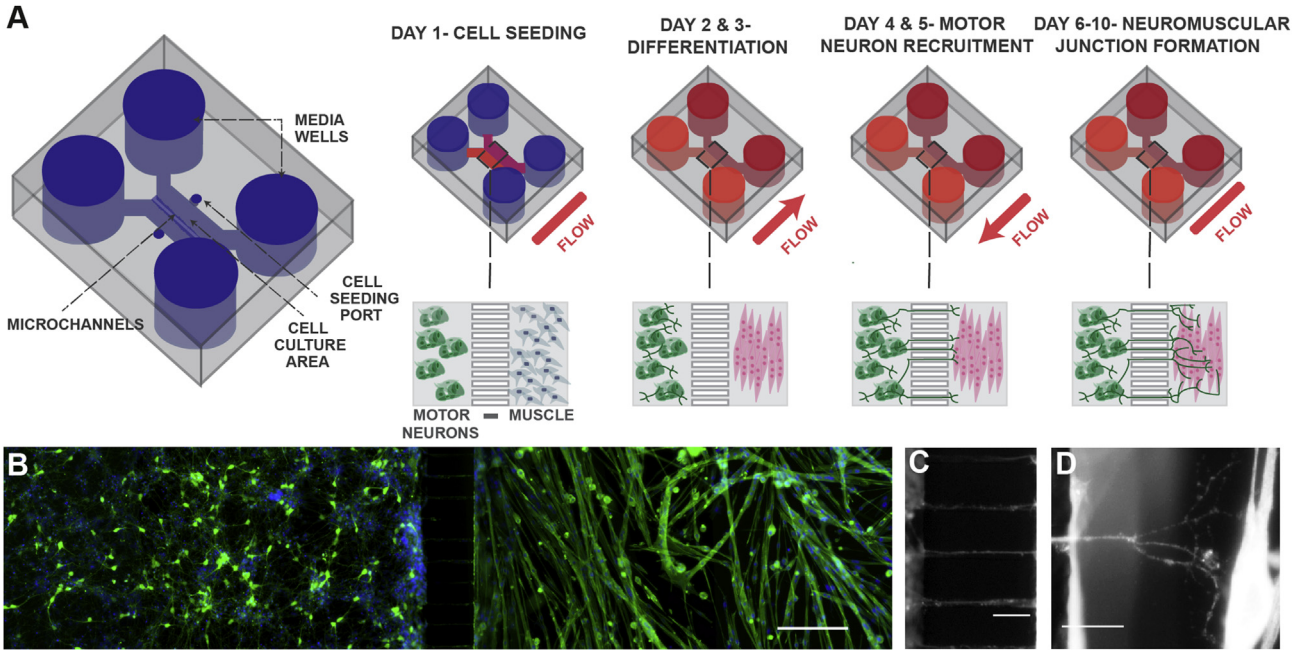

Figure 1: Schematic of neuromuscular junction microfluidic device. A) Primary myoblasts and mouse embryonic stem cell-derived motor neurons were seeded in separate cell culture compartments in a microfluidic device via the cell seeding ports. Myoblasts were then differentiated (over two days), forming multinucleated myofibers. During this period, motor neurons were kept fluidically isolated. Motor neuron processes were then recruited across the microchannel, via a chemotactic gradient of GDNF and BDNF (days 4 and 5) generated by small but sustained fluid flow from the muscle to the motor neuron compartment. NMJs were allowed to mature until day 10, under static conditions. B) Fluorescent image of microfluidic device showing motor neurons in the left-hand side compartment and muscle fibers in the right-hand side after 6 days of culture. Muscle fibers were stained for actin (green) and motor neurons were visualized by the Hb9:GFP reporter (green). Nuclei were stained with DAPI (blue). Scale bar represents 200 μm. C) A close-up fluorescent image of neurite processes crossing the central microchannels. Scale bar represents 50 μm. D) A close-up fluorescent image showing a neurite process extending, branching and contacting a muscle fiber. Scale bar represents 50 μm.

increase in myotube contraction was not the result of any direct action of KCl on myotubes. In response to tubocurarine treatment of the muscle compartment, myotubes in contact with motor neurons stopped contracting and became non-responsive to KCl treatment (Movie S4). Together, these results indicate the presence of functional NMJs in the microfluidic device.

Supplementary movie related to this article can be found at https://doi.org/10.1016/j.molmet.2017.11.001

3.2. Muscle PGC-1α1 promotes the recruitment of motor neurons

To investigate the roles of muscle PGC-1α1 and PGC-1α4 expression on NMJ formation, myotubes were transduced with recombinant adenoviruses expressing GFP and PGC-1α1 or GFP and PGC-1α4 from independent promoters (Figure 3*A-C*). As previously reported, overexpression of PGC-1α4, but not PGC-1α1, induced myotube hypertrophy [2] (Figure 3*B* and *C*). Control myotubes were transduced with an adenovirus expressing only GFP (Figure 3*D*). All myotube transductions were performed under fluidic isolation of the muscle compartment and adenovirus-driven expression of GFP was not observed within the motor neuron compartment. To confirm fluidic isolation during infection, we differentiated myoblasts into myotubes within both cell culture compartments, transduced one of the compartments under fluidic isolation and observed that only cells within the transduced compartment expressed GFP (Figure 3*D*). When robust expression of GFP was observed (one day after transduction), the muscle compartment was washed to remove residual virus and the fluid flow was reversed so that soluble factors secreted by the muscle could reach the neuronal compartment (Figure 3*A*). PGC-1α1 overexpression in myotubes resulted in a significant increase in motor neuron recruitment (3-fold when compared to GFP control), promoting the projection of axons into the muscle compartment (Figure 3*E*). Importantly, myotube PGC-1α1 expression resulted in levels of motor neuron recruitment that were comparable to those obtained following the addition of a combination of the chemoattractants BDNF and GDNF to the muscle compartment (Figure 2*A*). By contrast, PGC-1α4 did not cause a statistically significant increase in axonal projections across the microchannels (Figure 3*E*).

3.3. Expression of PGC-1α isoforms in muscle modulates NMJ morphology

To analyze NMJ morphology, we quantified the size of AChR aggregates in postsynaptic structures, identified as sites of colocalization of the AChR stain, α-bungarotoxin, with neurofilament immunolabeling. Overexpression of PGC-1α1 significantly increased the size of NMJs, with co-localization of AChR and motor neuron markers increasing 2.5-fold compared to GFP controls (Figure 3*F*). To determine whether PGC-1α1 or PGC-1α4 expression affected AChR clustering in general, we quantified the size and staining intensity of all AChR aggregates, including those that did not co-localize with neurofilament staining. Overexpression of PGC-1α4 led to significantly smaller AChR clusters, while PGC-1α1 expression led to greater AChR staining intensity (Figure 3G—*I*).

To investigate how changes in NMJ morphology affected function, we monitored spontaneous myotube contraction as well as contraction following motor neuron stimulation with KCl. After KCl stimulation, functional NMJs were confirmed by inhibition of myotube contraction with tubocurarine. Functional NMJs were found with both the GFP control and PGC-1α1 myotubes (Figure 3*J* and *K*). Moreover, PGC-1α1

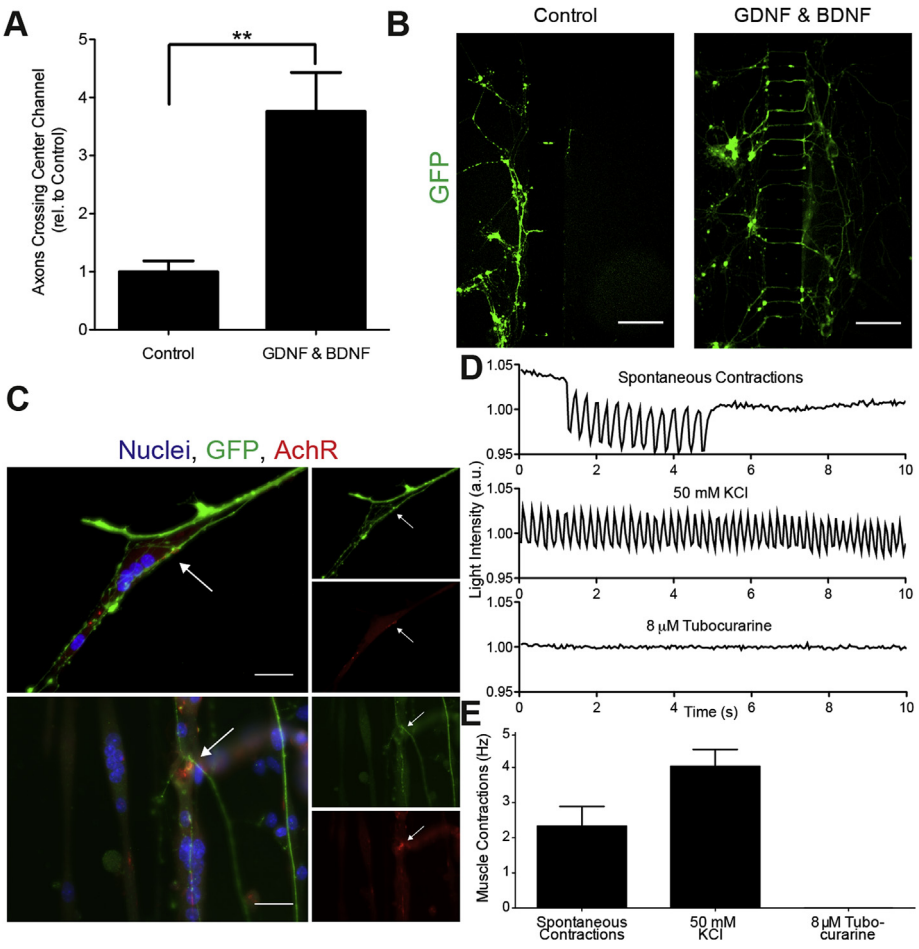

Figure 2: Neurotrophic factors, BDNF and GDNF, promote neuromuscular junction formation. A) Recruitment of neurite processes with and without growth factor recruitment (20 ng/ml of GDNF & BDNF) at day 6 of culture. Data presented as mean ± SEM relative to control for n = 6 experiments with 2–3 devices per condition of each experiment. Statistical significance was determined using a Student's t-test, (**) $p < 0.01$. B) Hb9-GFP positive motor neuron axons crossing center microchannels at day 6 with and without growth factor recruitment. Scale bars represent 200 μm. C) Immunolocalization of Hb9-positive motor neurons (green), acetylcholine receptors stained with α-bungarotoxin (red) and cell nuclei (blue). Arrows indicate NMJs. D) Myotube contractions (as measured by changes in light intensity) during normal culture conditions (spontaneous contractions), after motor neurons are treated with 50 mM KCl (induced contractions) and after inhibition of NMJs with 8 μM tubocurarine. E) Average frequency of spontaneous myotube contractions, after KCl stimulation of motor neurons, and after NMJ blocking with tubocurarine. Data is presented as mean ± SEM for n = 3 experiments.

myotubes showed fewer spontaneous contractions and a higher frequency of stimulated contraction upon KCl treatment of motor neurons. By contrast, no PGC-1α4 myotubes were observed to spontaneously contract or were responsive to motor neuron stimulation (Figure 3*L*). To understand these changes in contractility, intracellular calcium concentration was measured in GFP, PGC-1α1, and PGC-1α4 myotubes. Overexpression of PGC-1α1 caused myotube intracellular calcium levels to increase 1.25-fold, while PGC-1α4 caused calcium levels to decrease 1.2-fold compared to GFP controls (Figure S2). Together, this suggests that altered calcium handling may account for the changes in stimulated contractility observed within the *in vitro* NMJ model.

3.4. PGC-1α1 overexpression promotes retrograde signaling from muscle to motor neurons

Our finding that overexpression of PGC-1α1 in myotubes increased neuronal targeting to muscle suggests that muscle produces PGC-1α1-dependent soluble factors that mediate retrograde signaling from muscle to motor neurons. To confirm this, we prevented communication from myotubes to motor neurons by maintaining myotubes in fluidic isolation throughout culture, i.e., with flow from the neuron to the muscle compartment. Under these conditions, we observed no increase in axon recruitment across the microchannels when myotubes were transduced with the PGC-1α1 adenovirus (Figure 4*A*). These results indicate that soluble factors mediate the increase in neurite recruitment elicited by PGC-1α1 expression in muscle.

3.5. A genomics approach to identify putative PGC-1α1-dependent myokines

To identify potential PGC-1α1-regulated myokines, we examined gene expression data from myotubes overexpressing PGC-1α1 (published dataset, GEO GSE42473 [2]). Data were sequentially analyzed by the SignalP [19], TargetP [20], and Phobius [21] algorithms, to predict potential secreted factors. This approach identified 51 factors, which were validated by qRT-PCR, in myotubes overexpressing PGC-1α1 and in the quadriceps and gastrocnemius muscles of mice overexpressing PGC-1α1 specifically in skeletal muscle (MCK-PGC-1α1) (Figure S3). Based on known signaling roles and pathway analysis, three proteins were selected for further analysis; these included Interleukin 15 (IL-15), Neurturin (NRTN), and Nerve Growth Factor (NGF). NRTN and NGF were upregulated approximately 4-fold in myotubes overexpressing

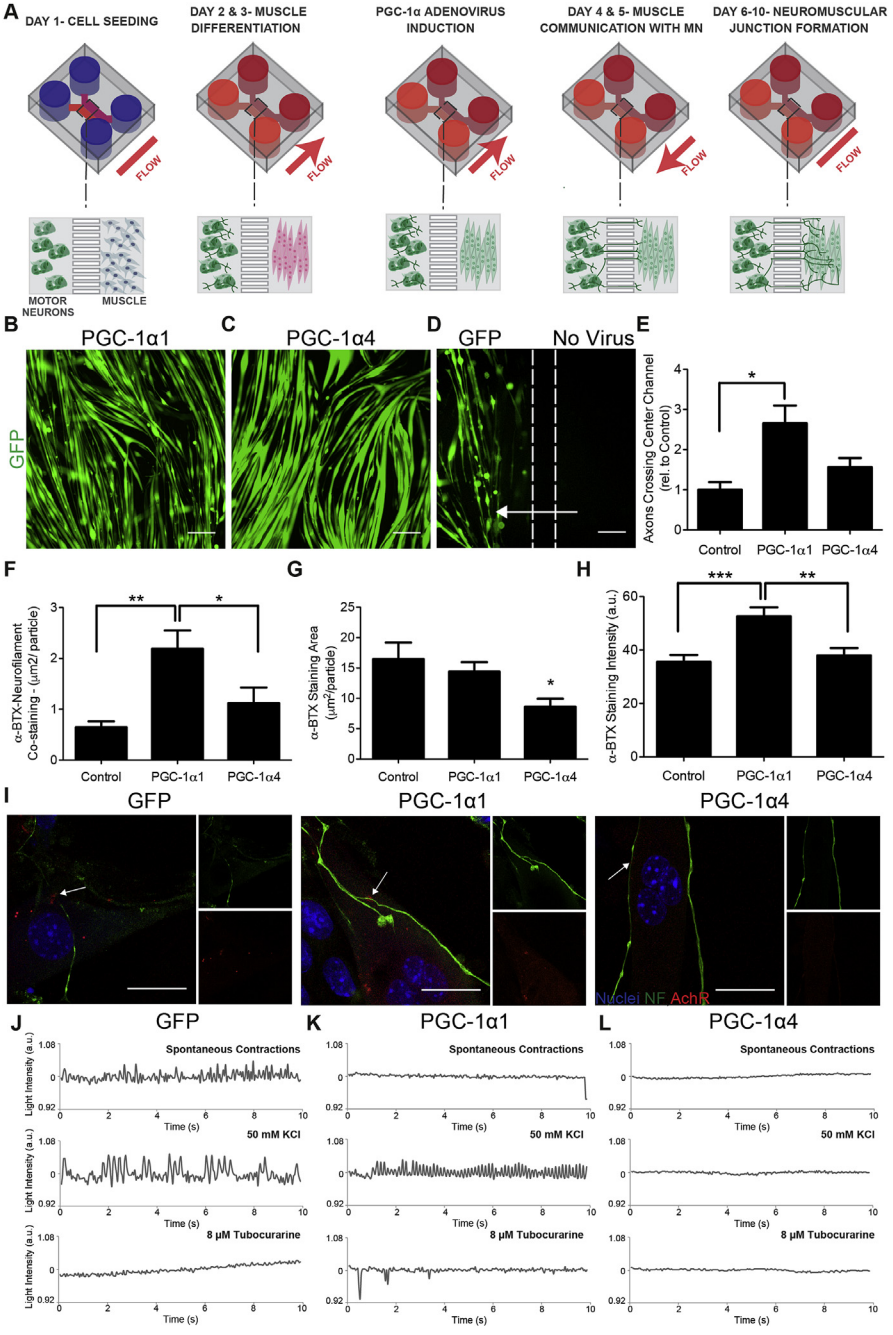

Figure 3: Expression of PGC-1α isoforms in muscle modulates axonal recruitment and NMJ morphology. A) Schematic of NMJ model with forced expression of PGC-1α1, PGC-1α4 and GFP. Experimental set-up was the same as in Figure 1 with the additional step of PGC-1α/GFP adenovirus transduction. After myotube differentiation, expression of PGC-1α1, PGC-1α4, and GFP was induced via an 8-hour viral transduction. During this time, media flow was directed from the motor neurons towards the muscle, fluidically isolating the myotubes and restricting the adenovirus to the muscle compartment. After virus transduction, muscle cells were washed and the media flow was reversed, flowing from the muscle side towards the motor neurons, allowing the muscle to 'communicate' with the motor neurons (days 4 & 5). Expression of B) PGC-1α1 and C) PGC-1α4 in myotubes using adenovirus induction. Scale bars represent 200 μm in B–D. D) Myoblasts were seeded and differentiated within both cell culture compartments, and GFP control adenovirus was added to one compartment (left side), while the flow was tailored towards the treated side (arrow). Only the treated compartment expressed GFP, demonstrating fluidic isolation during virus transduction. Dashed lines represent the approximate location of the microchannels. E) Motor neuron recruitment in response to overexpression of PGC-1α1, PGC-1α4 and GFP in myotubes. Data quantifies the number of axons crossing central channel at day 6 and is presented as mean ± SEM relative to GFP control for n = 4 experiments with 2–3 devices per condition of each experiment. Statistical significance was determined using one-way ANOVA with Bonferroni's post-hoc test, (*) $p < 0.05$. F) Mean area of co-staining of neurofilament and α-bungarotoxin (α-BTX), G) mean area of AchR clusters as determined by α-BTX staining, and H) mean intensity of α-BTX staining. Data represents mean ± SEM for n = 3 experiments. Statistical significance was determined using a Kruskal–Wallis test with Dunn's post-hoc test, (**) $p < 0.01$, (***) $p < 0.001$. I) Immunolocalization of neurofilament (NF) (green), AchR stained with α-BTX (red) and cell nuclei (blue). Smaller images show neurofilament (top) and α-BTX (bottom) staining individually. Arrows indicate NMJs. Scale bar represents 20 μm. Functional analysis of NMJ formation after myotubes were treated with J) GFP control, K) PGC-1α1 and L) PGC-1α4 adenoviruses. Graphs show muscle fibre contractions (as measured by changes in light intensity) during standard culture (spontaneous contractions), after motor neuron stimulation with 50 mM KCl, and after NMJ inhibition with 8 μM tubocurarine.

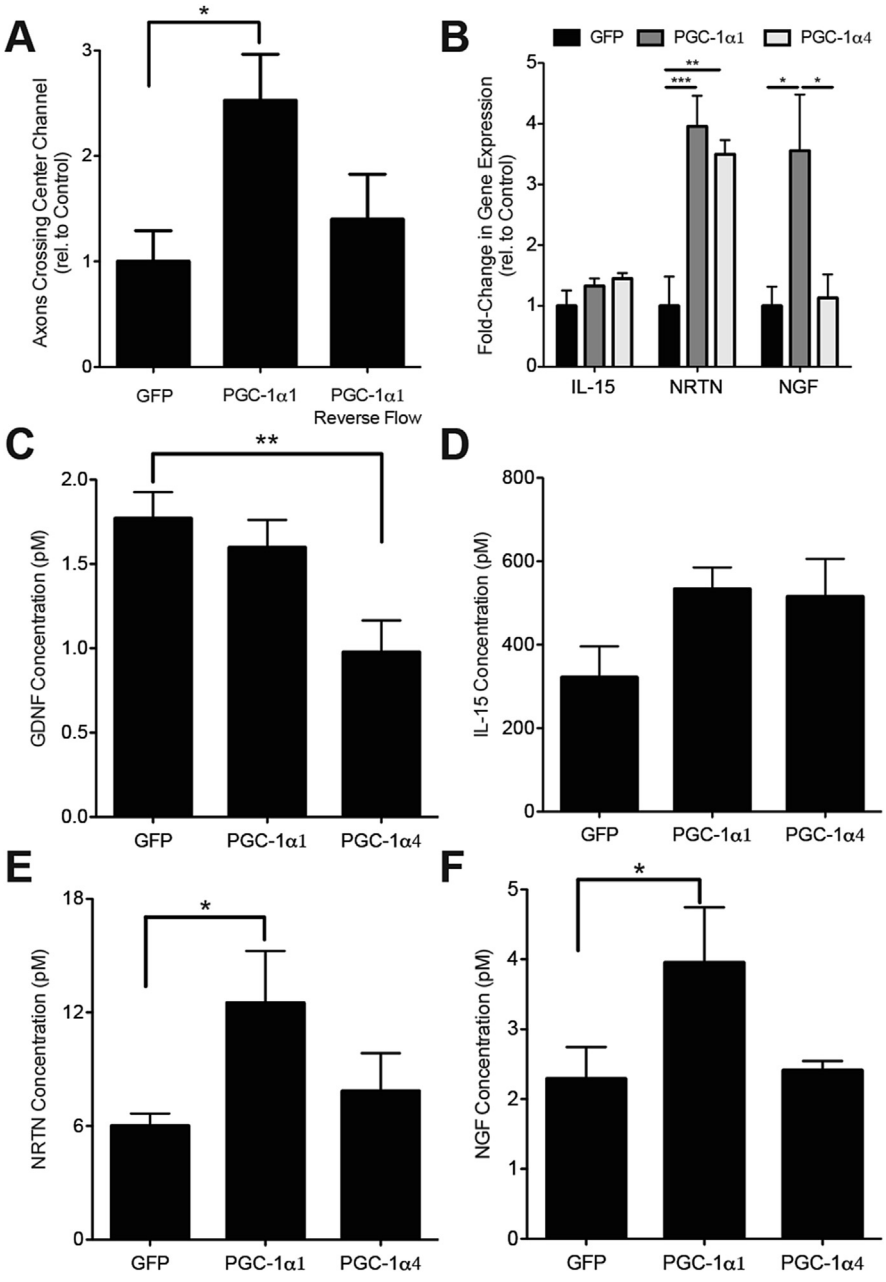

Figure 4: Soluble signals mediate PGC-1α1-associated motor neuron recruitment. A) Motor neuron recruitment in response to overexpression of PGC-1α1 at day 6 using standard flow (from muscle to motor neuron compartment) and reverse flow (from motor neuron to muscle compartment) on days 4 and 5. Data are presented as mean ± SEM relative to control for n = 3 experiments with 2–3 devices per condition of each experiment. B) Expression by RT-qPCR of interleukin 15 (IL-15), neurturin (NRTN) and nerve growth factor (NGF), relative to controls from myotubes overexpressing PGC-1α1 or PGC-1α4. Data are presented as mean ± SEM from n = 3 experiments. Statistical significance was determined using a one-way ANOVA with Bonferroni's post-hoc test, (***) $p < 0.001$, (**) $p < 0.01$, (*) $p < 0.05$. C–F) Factors secreted from myotubes in response to overexpression of PGC-1α1, PGC-1α4 and GFP. Concentration of C) glial derived neurotrophic factor (GDNF), D) interleukin 15 (IL-15), E) neurturin (NRTN), and F) nerve growth factor (NGF) within myotube cell culture medium was determined using a ProSeek assay. Data is presented as mean ± SEM from n = 3 experiments. Statistical significance was determined using a one-way ANOVA with Bonferroni's post-hoc test, (*) $p < 0.05$.

PGC-1α1, while NRTN gene-expression was also observed to increase in PGC-1α4 overexpressing myotubes (Figure 4*B*). Glial cell-derived neurotrophic factor (GDNF), a close relative of NRTN, was also included although it was not detected by our bioinformatics approach. To investigate the presence of secreted GDNF, IL-15, NRTN, and NGF in the myotube culture media, we used Proximity Extension Assays [22], which allow for quantitative protein detection with a qPCR readout and require low sample volumes (Figure S4). One microliter of media was taken from the muscle compartment of the devices to determine the levels of GDNF, IL-15, NRTN, and NGF secretion from myotubes in response to expression of PGC-1α1, PGC-1α4, and GFP. GDNF was secreted by the myotubes at low levels (1.7 pM) in GFP controls and was further reduced in muscle expressing PGC-1α4 (Figure 4*C*). IL-15 secretion was not significantly changed in either PGC-1α1- or PGC-1α4-expressing myotubes compared to those expressing GFP (Figure 4*D*). Consistent with our bioinformatics predictions, NRTN and

NGF secretion increased in PGC-1α1 expressing myotubes compared to GFP controls (Figure 4*E*, *F*). In contrast, PGC-1α4 expressing myotubes did not show increased secretion of NRTN (in contrast to gene expression data) or NGF compared to GFP expressing myotubes.

3.6. Neurturin is a key component of PGC-1α1-mediated motor neuron recruitment

To investigate the capacity of NRTN and NGF to recruit neurites, we added recombinant NRTN or NGF to the myotube compartment following muscle differentiation and quantified the numbers of neurites crossing the center of the microchannels. NGF did not have an effect on neurite recruitment. In contrast, NRTN led to a significant increase in neurite recruitment (6-fold) compared to control conditions where no growth factors were added (Figure 5*A*). To confirm that Hb9:GFP motor neurons were competent to respond to NRTN, expression of the NRTN receptor, GDNF family receptor α2 (GFRα2) [23], was measured by qRT-PCR. The increase in GFP during motor neuron patterning (Figure 5*B*) coincided with a 3-fold increase in GFRα2 expression (Figure 5*C*), suggesting that Hb9-GFP motor neurons were able to sense extracellular NRTN.

To investigate whether NRTN is necessary for enhanced neurite recruitment downstream of PGC-1α1, myotubes were sequentially transduced on days three and four with adenoviruses expressing NRTN shRNA (Vector Biolabs) or a scrambled shRNA control (Vector Biolabs) and PGC-1α1 or GFP control (Figure S5). Silencing NRTN gene expression prevented the enhanced neurite recruitment observed with PGC-1α1 expression in muscle (Figure 5*D*). Together, these results suggest that NRTN mediates PGC-1α1-associated signaling from muscle to motor neurons.

Given that NRTN secretion increases with PGC-1α1 expression *in vitro* (Figure 4*E*) and is sufficient (Figure 5*A*) and necessary (Figure 5*D*) for PGC-1α1-mediated neurite recruitment, we investigated whether NRTN expression correlated with PGC-1α1 levels *in vivo*. Gastrocnemius muscles were collected from mice overexpressing PGC-1α1 in skeletal muscle [24] and from muscle-specific PGC-1α knockout mice [25] and NRTN expression was measured by qRT-PCR. The muscles from mice overexpressing PGC-1α1 showed a substantial increase in NRTN expression (6-fold) (Figure 5*C*) compared to wild-type littermates, while muscle-specific knockout of PGC-1α resulted in a more than 2-fold decrease in NRTN expression (Figure 5*D*).

4. DISCUSSION

Physical activity is known to confer protective properties against sarcopenia and many neurodegenerative diseases [26,27]. PGC-1α transcriptional coactivators are induced by exercise in skeletal muscle and cause many of the adaptations associated with endurance exercise (PGC-1α1) and resistance training (PGC-1α4) [2]. The NMJ acts as an interface between the nervous and skeletal muscle systems, receiving inputs from pre- and post-synaptic origins, and has been observed to have a high morphological and functional plasticity [27–30]. Increasing evidence highlights the contribution of skeletal muscle to the maintenance and remodeling of the NMJ [7,10,31,32]. In this study, we investigated the effect of PGC-1α1 and PGC-1α4 on NMJ formation and maintenance using an *in vitro* NMJ model and explored the factors responsible for PGC-1α1-mediated retrograde signaling.

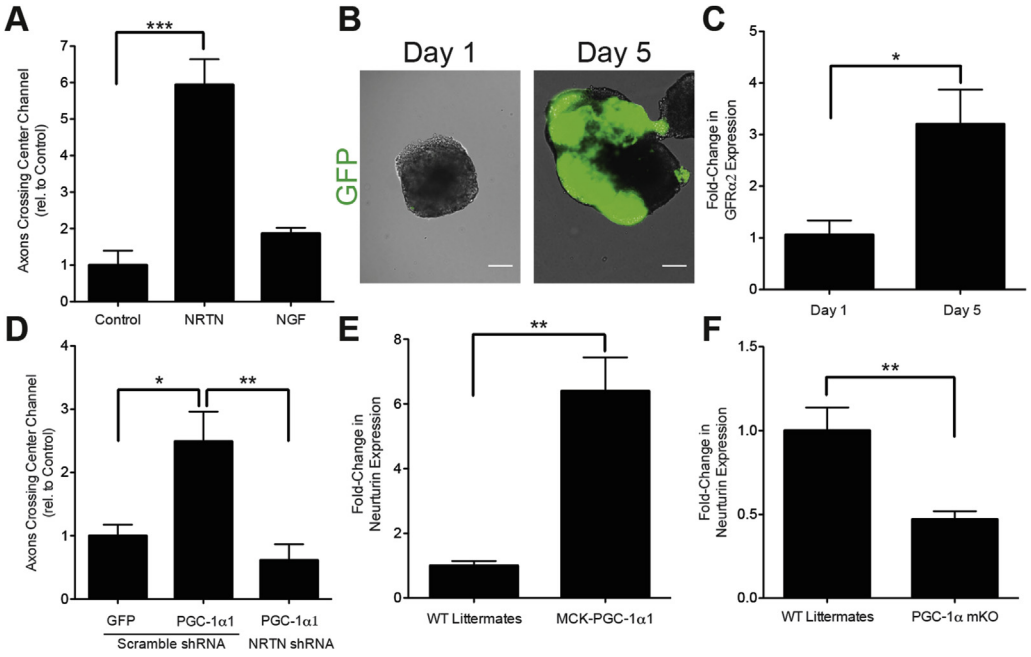

Figure 5: Neurturin is a key component of PGC-1α1-mediated motor neuron recruitment. A) Recruitment of axons using recombinant NRTN and NGF at day 6 of culture. Data is presented as mean ± SEM relative to control for n = 2 experiments with 2–3 devices per condition of each experiment. Statistical significance was determined using a one-way ANOVA with Bonferroni's post-hoc test (***) $p < 0.001$. B) Hb9-GFP embryoid bodies on days 1 and 5 of motor neuron differentiation. Scale bar represents 100 μm. C) GDNF-family receptor α2 expression, as determined by qRT-PCR, in Hb9-GFP embryoid bodies on days 1 and 5 of motor neuron differentiation. Data is presented as mean ± SEM relative to day 1 for n = 3 experiments. Statistical significance was determined using a t-test (*) $p < 0.05$. D) Axon recruitment at day 6 of culture in response to overexpression of PGC-1α1 with shRNA inhibition of NRTN. Data is presented as mean ± SEM relative to GFP control for n = 2 experiments with 3–4 devices per condition of each experiment. NRTN expression, as determined by qRT-PCR, in the gastrocnemius muscles of E) mice overexpressing PGC-1α1 in skeletal muscle (MCK-PGC-1α1) and F) muscle-specific PGC-1α knockout mice (PGC-1α mKO), compared to wild type (WT) littermates. Data is presented as mean ± SEM relative to WT littermates control for n = 4 WT animals, n = 6 MCK-PGC1α1 animals, and n = 6 PGC-1α mKO animals.

PGC-1α1 expression in skeletal muscle has been associated with pre- and post-synaptic remodeling of the NMJ, mimicking the effects of physical exercise [7]. For example, PGC-1α1 expression in skeletal muscle causes lengthening and branching of motor axons while decreasing the number of axons that do not terminate in a NMJ [7]. Furthermore, muscle-specific PGC-1α1 expression converts muscle to a slow phenotype [24] and is associated with increased expression of SV2A in motor neuron terminals, a marker for slow motor neurons [10]. NMJ deficits have not been described for muscle-specific PGC-1α1 knockout animals, although results linking PGC-1α1 to the formation of aneural AChR clusters [8] and increased NMJ size and integrity [7] suggest that PGC-1α1 may play an important role in NMJ adaptation to postnatal challenges (e.g. injury, exercise, aging). In addition, muscle-specific PGC-1α1 knockout animals show a compensatory PGC-1β elevation in skeletal muscle, especially at young ages [33]. In line with this, gene array data from transgenic mice expressing PGC-1β in skeletal muscle show a 5-fold increase in NRTN expression (ArrayExpress E-MEXP-939) [34]. However, no myokines under the control of PGC-1α1 have been previously identified in PGC-1α1-driven NMJ retrograde signaling.

Within our microfluidic NMJ model, expression of PGC-1α1 in skeletal muscle resulted in increased neuronal recruitment, larger NMJs, and brighter staining of aneural AChRs, in agreement with previous findings [7,8]. The increased neurite recruitment in particular suggests that PGC-1α1 controls the expression of muscle-derived neurotrophic factors that mediate retrograde signaling to motor neurons. Importantly, our microfluidic model allowed us to control the direction of paracrine signaling between neurons and muscle and thereby demonstrate that a muscle-derived soluble factor(s) was responsible for the neuronal recruitment observed. Our finding that PGC-1α4 did not affect neurite recruitment, AChR staining intensity, or NMJ size suggests that hypertrophic adaption to resistance training is independent from NMJ recruitment. In fact, AChR clusters were smaller and calcium levels decreased in response to PGC-1α4 expression. Taken together, this suggests PGC-1α4 may initiate a process of NMJ selection and altered muscle excitability that could be important during adaptation to resistance training.

While a number of retrograde signals have been identified during NMJ development, very little is known about retrograde mediators of NMJ plasticity during adaptation to exercise [7,31,35]. We used a bioinformatics approach to identify 51 potential secreted factors upregulated after overexpression of PGC-1α1 and chose four factors to examine in detail, GDNF, IL-15, NRTN, and NGF. GDNF was not identified in the initial bioinformatics screen but was also included as it has been previously shown to be induced by physical activity [36–38] and has a prominent role in motor neuron survival and NMJ maturation [35,39]. Three of the factors (GDNF, NRTN, and NGF) were secreted at different concentrations in response to PGC-1α1 and PGC-1α4 expression, showing that myokine secretion can be PGC-1α isoform specific. Interestingly, NRTN gene expression increased in response to both PGC-1α1 and PGC-1α4 overexpression, but increased NRTN secretion was specific to PGC-1α1. This result points to changes in post-transcriptional mRNA processing and post-translational protein modifications that can affect protein secretion and are PGC-1α isoform specific [40]. Importantly, exogenous NRTN could phenocopy the effects of PGC-1α1 overexpression on neurite recruitment and NRTN inhibition via shRNA returned neurite recruitment to control levels. Together these results suggest that NRTN is a key retrograde factor responsible for the pre-synaptic effects observed after PGC-1α1 muscle overexpression within our system.

NRTN is a member of the GDNF family of neurotrophic factors that also includes GDNF, persephin, and artemin [41,42]. These proteins are potent survival and maturation signals for various neuronal populations [43]. In muscle, NRTN induces AChRs to become localized to the surface membrane and form clusters [44]. In motor neurons, NRTN causes neurite growth and microtubule assembly through GFRα2-mediated MAPK and Src-kinase signaling [23]. Addition of NRTN to xenopus nerve-muscle co-cultures causes presynaptic changes, increasing axonal growth within 24 h of treatment [45]. During postnatal development in mice, neurturin expression in pilo-erection muscles directly correlates with muscle innervation [46], in agreement with our findings that NRTN is a mediator of retrograde signaling between muscle and motor neurons. Interestingly, a NMJ phenotype has not been described in NRTN knockout animals, although they do exhibit a substantial reduction in cholinergic innervation in the heart [47]. This result suggests that other GDNF family ligands may act redundantly to facilitate NMJ formation during development. Accordingly, knockout of the RET tyrosine kinase receptor, a general receptor for GDNF family ligands, causes severe deficits in motor neuron maturation during development and regeneration [48].

In human skeletal muscle, a single bout of exercise stimulates a pulse of PGC-1α expression [49], providing a parallel to the adenovirus-mediated PGC-1α1 expression in our *in vitro* system. In a cohort of 49 male and female subjects aged 18–80, NRTN gene expression significantly correlates with PGC-1α expression prior to exercise intervention ($p = .016$, $r^2 = .113$) (GEO GSE8479) [50]. After 12 weeks of exercise intervention in the older cohort, NRTN expression in skeletal muscle increased significantly ($p = .005$) compared to baseline [50]. Together, this suggests a relationship between PGC-1α and NRTN expression in human skeletal muscle and a potential mechanism for linking exercise to changes in NMJs.

To understand the mechanisms of PGC-1α1-associated increases in NRTN expression, we examined predicted transcription factor binding sites within the mouse NRTN promoter. Interestingly, Yin Yang 1 (YY1) had three predicted binding sites in the NRTN promoter region and PGC-1α has been shown to act as a co-activator with YY1 to promote expression of other genes involved in muscle adaptation [51]. YY1 has also been shown by ChIP-seq to bind to the neurturin promoter region in mouse myoblasts (ch17:56904570 – ch17:56904682, Qvalue = 1e-5.32) (GSE45875 [52]) and mouse muscle-specific knockout of YY1 results in decreased PGC-1α and NRTN expression [53]. Taken together, these results suggest that YY1 may play a role in PGC-1α1 regulation of NRTN.

Our work suggests that NRTN is involved in PGC-1α1 mediated neuronal recruitment and myotube innervation. This has potential applications in the development of treatment strategies for neurodegenerative diseases, including amyotrophic lateral sclerosis (ALS) and spinal muscular atrophy, where NMJs are early pathological targets [54]. Muscle-specific PGC-1α1 overexpression in mice has been shown to improve muscle function in models of Duchenne muscular dystrophy [8] and ALS [55]. Therefore, NRTN modulation in neuromuscular diseases has translational potential.

The concept of skeletal muscle exerting endocrine functions through myokines is becoming increasingly recognized [56,57]. The use of a PGC-1α genetic model isolates the direct effects of skeletal muscle conditioning and provides a simple method to analyze 'exercise myokines'. Additionally, the use of microfluidic systems allows for improved control over the cellular microenvironment. Here we integrate these systems to gain new insights into the biology of PGC-1α. Further investigation of PGC-1α mediated myokines will have important implications in understanding how exercise improves overall organism health and provide new avenues for pharmacological targets to treat numerous chronic diseases.

5. CONCLUSION

We used a microfluidic system to model endocrine signaling and NMJ formation between skeletal muscle and motor neurons. Using this system, we showed that muscle PGC-1α1, but not PGC-1α4, promotes neurite recruitment and larger NMJs. Neurturin appears to mediate these effects since muscle PGC-1α1 stimulates neurturin secretion and neurturin is sufficient and necessary for the improved NMJ formation. Our findings point to neurturin as a novel mediator of PGC-1α1-dependent retrograde signaling from skeletal muscle to motor neurons.

CONFLICT OF INTEREST

None declared.

ACKNOWLEDGMENTS

The mHb9:GFP mESC line was kindly provided by the Stem Cell Core Facility at the Columbia University Stem Cell Initiative. This work was supported by grants from the Human Frontier Science Program Young Investigator Award (JLR and AIT) (RGY0082-2014), the Whitaker International Program (HT-W), the Wenner-Gren Foundation post-doctoral fellowship (DMSF), the Åke Wiberg Stiftelse (AIT), and the Strategic Research Area in Stem Cell Research and Regenerative Medicine at Karolinska Institutet (JLR and AIT). Additional support was provided by the Swedish Medical Research Council (EH) (2016-02112), the Joint Program for Neurodegenerative Diseases (EH) (529-2014-7500), the Åhlén-stiftelsen (mA1/h15), Birgit Backmark's Donation to ALS research at Karolinska Institutet in memory of Nils and Hans Backmark (EH), Magnus Bergvalls stiftelse (2015-00783) and the Strategic Research Area in Neuroscience at Karolinska Institutet (StratNeuro) (EH). JCC is recipient of a postdoctoral fellowship from the Swedish Society for Medical Research (SSMF).

APPENDIX A. SUPPLEMENTARY DATA

Supplementary data related to this article can be found at https://doi.org/10.1016/j.molmet.2017.11.001

REFERENCES

[1] Lin, J., Handschin, C., Spiegelman, B.M., 2005. Metabolic control through the PGC-1 family of transcription coactivators. Cell Metabolism 1(6):361—370.

[2] Ruas, J.L., White, J.P., Rao, R.R., Kleiner, S., Brannan, K.T., Harrison, B.C., et al., 2012. A PGC-1 alpha isoform induced by resistance training regulates skeletal muscle hypertrophy. Cell 151(6):1319—1331.

[3] Puigserver, P., Wu, Z.D., Park, C.W., Graves, R., Wright, M., Spiegelman, B.M., 1998. A cold-inducible coactivator of nuclear receptors linked to adaptive thermogenesis. Cell 92(6):829—839.

[4] Zhang, Y.B., Huypens, P., Adamson, A.W., Chang, J.S., Henagan, T.M., Boudreau, A., et al., 2009. Alternative mRNA splicing produces a novel biologically active short isoform of PGC-1 alpha. Journal of Biological Chemistry 284(47):32813—32826.

[5] Miura, S., Kai, Y., Kamei, Y., Ezaki, O., 2008. Isoform-specific increases in murine skeletal muscle peroxisome proliferator-activated receptor-gamma coactivator-1 alpha (PGC-1 alpha) mRNA in response to beta 2-adrenergic receptor activation and exercise. Endocrinology 149(9):4527—4533.

[6] Arany, Z., 2008. *PGC*-1 coactivators and skeletal muscle adaptations in health and disease. Current Opinion in Genetics & Development 18(5):426—434.

[7] Arnold, A.S., Gill, J., Christe, M., Ruiz, R., McGuirk, S., St-Pierre, J., et al., 2014. Morphological and functional remodelling of the neuromuscular junction by skeletal muscle PGC-1alpha. Nature Communications 5:3569.

[8] Handschin, C., Kobayashi, Y.M., Chin, S., Seale, P., Campbell, K.P., Spiegelman, B.M., 2007. PGC-1α regulates the neuromuscular junction program and ameliorates Duchenne muscular dystrophy. Genes & Development 21(7):770—783.

[9] Sandri, M., Lin, J., Handschin, C., Yang, W., Arany, Z.P., Lecker, S.H., et al., 2006. PGC-1α protects skeletal muscle from atrophy by suppressing FoxO3 action and atrophy-specific gene transcription. Proceedings of the National Academy of Sciences 103(44):16260—16265.

[10] Chakkalakal, J.V., Nishimune, H., Ruas, J.L., Spiegelman, B.M., Sanes, J.R., 2010. Retrograde influence of muscle fibers on their innervation revealed by a novel marker for slow motoneurons. Development 137(20):3489—3499.

[11] Sackmann, E.K., Fulton, A.L., Beebe, D.J., 2014. The present and future role of microfluidics in biomedical research. Nature 507(7491):181—189.

[12] Zahavi, E.E., Ionescu, A., Gluska, S., Gradus, T., Ben-Yaakov, K., Perlson, E., 2015. Spatial aspects of GDNF functions revealed in a compartmentalized microfluidic neuromuscular co-culture system. Journal of Cell Science 128:1241—1252.

[13] Di Giorgio, F.P., Carrasco, M.A., Siao, M.C., Maniatis, T., Eggan, K., 2007. Non-cell autonomous effect of glia on motor neurons in an embryonic stem cell-based ALS model. Nature Neuroscience 10(5):608—614.

[14] Wichterle, H., Lieberam, I., Porter, J.A., Jessell, T.M., 2002. Directed differentiation of embryonic stem cells into motor neurons. Cell 110(3):385—397.

[15] Taylor, A.M., Blurton-Jones, M., Rhee, S.W., Cribbs, D.H., Cotman, C.W., Jeon, N.L., 2005. A microfluidic culture platform for CNS axonal injury, regeneration and transport. Nature Methods 2(8):599—605.

[16] Emanuelsson, O., Brunak, S., von Heijne, G., Nielsen, H., 2007. Locating proteins in the cell using TargetP, SignalP and related tools. Nature Protocols 2(4):953—971.

[17] Allodi, I., Hedlund, E., 2014. Directed midbrain and spinal cord neurogenesis from pluripotent stem cells to model development and disease in a dish. Frontiers in Neuroscience 8.

[18] Yuan, X.B., Jin, M., Xu, X.H., Song, Y.Q., Wu, C.P., Poo, M.M., et al., 2003. Signalling and crosstalk of Rho GTPases in mediating axon guidance. Nature Cell Biology 5(1):38—45.

[19] Petersen, T.N., Brunak, S., von Heijne, G., Nielsen, H., 2011. SignalP 4.0: discriminating signal peptides from transmembrane regions. Nature Methods 8(10):785—786.

[20] Emanuelsson, O., Nielsen, H., Brunak, S., von Heijne, G., 2000. Predicting subcellular localization of proteins based on their N-terminal amino acid sequence. Journal of Molecular Biology 300(4):1005—1016.

[21] Kall, L., Krogh, A., Sonnhammer, E.L., 2004. A combined transmembrane topology and signal peptide prediction method. Journal of Molecular Biology 338(5):1027—1036.

[22] Jarvius, M., Paulsson, J., Weibrecht, I., Leuchowius, K.-J., Andersson, A.-C., Wählby, C., et al., 2007. In situ detection of phosphorylated platelet-derived growth factor receptor β using a generalized proximity ligation method. Molecular & Cellular Proteomics 6(9):1500—1509.

[23] Wanigasekara, Y., Keast, J.R., 2005. Neurturin has multiple neurotrophic effects on adult rat sacral parasympathetic ganglion neurons. European Journal of Neuroscience 22(3):595—604.

[24] Lin, J., Wu, H., Tarr, P.T., Zhang, C.-Y., Wu, Z., Boss, O., et al., 2002. Transcriptional co-activator PGC-1[alpha] drives the formation of slow-twitch muscle fibres. Nature 418(6899):797—801.

[25] Chinsomboon, J., Ruas, J., Gupta, R.K., Thom, R., Shoag, J., Rowe, G.C., et al., 2009. The transcriptional coactivator PGC-1 alpha mediates exercise-induced angiogenesis in skeletal muscle. Proceedings of the National Academy of Sciences of the United States of America 106(50):21401—21406.

[26] Kaspar, B.K., Frost, L.M., Christian, L., Umapathi, P., Gage, F.H., 2005. Synergy of insulin-like growth factor-1 and exercise in amyotrophic lateral sclerosis. Annals of Neurology 57(5):649—655.

[27] Rudolf, R., Khan, M.M., Labeit, S., Deschenes, M.R., 2014. Degeneration of neuromuscular junction in age and dystrophy. Frontiers in Aging Neuroscience 6.
[28] Tsai, P.I., Wang, M.Y., Kao, H.H., Cheng, Y.J., Lin, Y.J., Chen, R.H., et al., 2012. Activity-dependent retrograde laminin A signaling regulates synapse growth at Drosophila neuromuscular junctions. Proceedings of the National Academy of Sciences of the United States of America 109(43):17699–17704.
[29] Berke, B., Wittnam, J., McNeill, E., Van Vactor, D.L., Keshishian, H., 2013. Retrograde BMP signaling at the synapse: a permissive signal for synapse maturation and activity-dependent plasticity. Journal of Neuroscience 33(45): 17937–17950.
[30] Yumoto, N., Kim, N., Burden, S.J., 2012. Lrp4 is a retrograde signal for presynaptic differentiation at neuromuscular synapses. Nature 489(7416):438.
[31] Taetzsch, T., Tenga, M.J., Valdez, G., 2017. Muscle fibers secrete FGFBP1 to slow degeneration of neuromuscular synapses during aging and progression of ALS. Journal of Neuroscience 37(1):70–82.
[32] Wu, H.T., Barik, A., Lu, Y.S., Shen, C.Y., Bowman, A., Li, L., et al., 2015. Slit2 as a beta-catenin/Ctnnb1-dependent retrograde signal for presynaptic differentiation. Elife 4.
[33] Sczelecki, S., Besse-Patin, A., Abboud, A., Kleiner, S., Laznik-Bogoslavski, D., Wrann, C.D., et al., 2014. Loss of Pgc-1 alpha expression in aging mouse muscle potentiates glucose intolerance and systemic inflammation. American Journal of Physiology-Endocrinology and Metabolism 306(2):E157–E167.
[34] Arany, Z., Lebrasseur, N., Morris, C., Smith, E., Yang, W.L., Ma, Y.H., et al., 2007. The transcriptional coactivator PGC-1 beta drives the formation of oxidative type IIX fibers in skeletal muscle. Cell Metabolism 5(1):35–46.
[35] Paratcha, G., Ledda, F., 2008. GDNF and GFRα: a versatile molecular complex for developing neurons. Trends in Neurosciences 31(8):384–391.
[36] Gyorkos, A.M., McCullough, M.J., Spitsbergen, J.M., 2014. Glial cell line-derived neurotrophic factor (GDNF) expression and NMJ plasticity in skeletal muscle following endurance exercise. Neuroscience 257(0):111–118.
[37] Gyorkos, A.M., Spitsbergen, J.M., 2014. GDNF content and NMJ morphology are altered in recruited muscles following high-speed and resistance wheel training. Physiological Reports 2(2).
[38] McCullough, M.J., Peplinski, N.G., Kinnell, K.R., Spitsbergen, J.M., 2011. Glial cell line-derived neurotrophic factor protein content in rat skeletal muscle is altered by increased physical activity in vivo and in vitro. Neuroscience 174(0): 234–244.
[39] Kanning, K.C., Kaplan, A., Henderson, C.E., 2010. Motor neuron diversity in development and disease. Annual Review of Neuroscience 33(1):409–440.
[40] Martinez-Redondo, V., Jannig, P.R., Correia, J.C., Ferreira, D.M.S., Cervenka, I., Lindvall, J.M., et al., 2016. Peroxisome proliferator-activated receptor gamma coactivator-1 alpha isoforms selectively regulate multiple splicing events on target genes. Journal of Biological Chemistry 291(29): 15169–15184.
[41] Golden, J.P., DeMaro, J.A., Osborne, P.A., Milbrandt, J., Johnson Jr., E.M., 1999. Expression of neurturin, GDNF, and GDNF family-receptor mRNA in the developing and mature mouse. Experimental Neurology 158(2):504–528.
[42] Kotzbauer, P.T., Lampe, P.A., Heuckeroth, R.O., Golden, J.P., Creedon, D.J., Johnson, E.M., et al., 1996. Neurturin, a relative of glial-cell-line-derived neurotrophic factor. Nature 384(6608):467–470.
[43] Bilak, M.M., Shifrin, D.A., Corse, A.M., Bilak, S.R., Kuncl, R.W., 1999. Neuroprotective utility and neurotrophic action of neurturin in postnatal motor neurons: comparison with GDNF and persephin. Molecular and Cellular Neuroscience 13(5):326–336.
[44] Yang, L.X., Nelson, P.G., 2004. Glia cell line-derived neurotrophic factor regulates the distribution of acetylcholine receptors in mouse primary skeletal muscle cells. Neuroscience 128(3):497–509.
[45] Wang, C.-Y., Yang, F., He, X.-P., Je, H.-S., Zhou, J.-Z., Eckermann, K., et al., 2002. Regulation of neuromuscular synapse development by glial cell line-derived neurotrophic factor and neurturin. Journal of Biological Chemistry 277(12):10614–10625.
[46] Furlan, A., La Manno, G., Lubke, M., Haring, M., Abdo, H., Hochgerner, H., et al., 2016. Visceral motor neuron diversity delineates a cellular basis for nipple- and pilo-erection muscle control. Nature Neuroscience 19(10):1331–1340.
[47] Mabe, A.M., Hoover, D.B., 2009. Structural and functional cardiac cholinergic deficits in adult neurturin knockout mice. Cardiovascular Research 82(1):93–99.
[48] Baudet, C., Pozas, E., Adameyko, I., Andersson, E., Ericson, J., Ernfors, P., 2008. Retrograde signaling onto Ret during motor nerve terminal maturation. Journal of Neuroscience 28(4):963–975.
[49] Norheim, F., Langleite, T.M., Hjorth, M., Holen, T., Kielland, A., Stadheim, H.K., et al., 2014. The effects of acute and chronic exercise on PGC-1 alpha, irisin and browning of subcutaneous adipose tissue in humans. FEBS Journal 281(3):739–749.
[50] Melov, S., Tarnopolsky, M.A., Beckman, K., Felkey, K., Hubbard, A., 2007. Resistance exercise reverses aging in human skeletal muscle. Plos One 2(5).
[51] Cunningham, J.T., Rodgers, J.T., Arlow, D.H., Vazquez, F., Mootha, V.K., Puigserver, P., 2007. mTOR controls mitochondrial oxidative function through a YY1-PGC-1 alpha transcriptional complex. Nature 450(7170):736.
[52] Lu, L.N., Sun, K., Chen, X.N., Zhao, Y., Wang, L.J., Zhou, L., et al., 2013. Genome-wide survey by ChIP-seq reveals YY1 regulation of lincRNAs in skeletal myogenesis. The EMBO Journal 32(19):2575–2588.
[53] Blattler, S.M., Verdeguer, F., Liesa, M., Cunningham, J.T., Vogel, R.O., Chim, H., et al., 2012. Defective mitochondrial morphology and bioenergetic function in mice lacking the transcription factor Yin Yang 1 in skeletal muscle. Molecular and Cellular Biology 32(16):3333–3346.
[54] Comley, L.H., Nijssen, J., Frost-Nylen, J., Hedlund, E., 2016. Cross-disease comparison of amyotrophic lateral sclerosis and spinal muscular atrophy reveals conservation of selective vulnerability but differential neuromuscular junction pathology. Journal of Comparative Neurology 524(7):1424–1442.
[55] Da Cruz, S., Parone, Philippe A., Lopes, Vanda S., Lillo, C., McAlonis-Downes, M., Lee, Sandra K., et al., 2012. Elevated PGC-1α activity sustains mitochondrial biogenesis and muscle function without extending survival in a mouse model of inherited ALS. Cell Metabolism 15(5):778–786.
[56] Agudelo, Leandro Z., Femenía, T., Orhan, F., Porsmyr-Palmertz, M., Goiny, M., Martinez-Redondo, V., et al., 2014. Skeletal muscle PGC-1α1 modulates kynurenine metabolism and mediates resilience to stress-induced depression. Cell 159(1):33–45.
[57] Pedersen, B.K., Febbraio, M.A., 2012. Muscles, exercise and obesity: skeletal muscle as a secretory organ. Nature Reviews Endocrinology 8(8):457–465.

